Journal Name

Dalton Transactions

ARTICLE TYPE

Transmetalation from B to Rh in the course of the catalytic asymmetric 1,4-addition reaction of phenylboronic acid to enones: A computational comparison of diphosphane and diene ligands
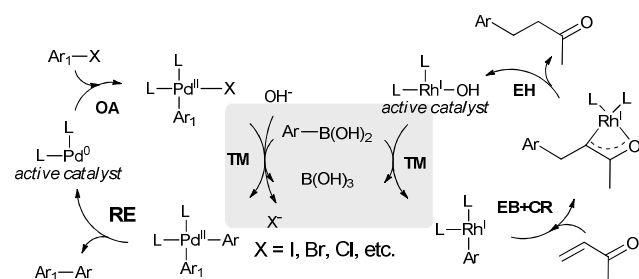
Yougui Li,*[a] Gang He,[a] Huali Qin[b] and Eric Assen B. Kantchev*[a,c]

Transmetalation is a key elementary reaction of many important catalytic reactions. Among those, the 1,4-addition of arylboronic acids to organic acceptors such as α,β-unsaturated ketones has emerged as one of the most important methods for asymmetric C-C bond formation. A key intermediate for the B-to-Rh transfer arising from quaternization on the boronic acid by a Rh-bound hydroxide (the active catalyst) has been proposed. Herein, DFT calculations (IEFPCM/PBE0/DGDZVP level of theory) establish the viability of this proposal, and characterize the associated pathways. The delivery of the phenylboronic acid in the orientation suited for the B-to-Rh transfer from the very beginning is energetically preferable, and occurs with expulsion of Rh-coordinated water molecules. For the bulkier binap ligand, the barriers are higher (particularly for the phenylboronic acid activation step) due to a less favourable entropy term to the free energy, in accordance with the experimentally observed slower transmetalation rate.
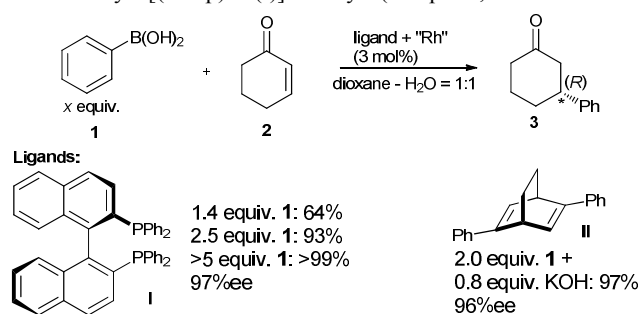
Introduction

Among organoboron compounds, boronic acids[1] have become the most prominent choice for uses in catalysis[2] due to their easy accessibility, air- and moisture-tolerance and low toxicity. The key elementary reaction that enables such applications is transmetalation (TM) from B to the catalytically active transition metal.[3] For instance, in the Nobel Prize-winning Suzuki-Miyaura reaction[4] (Scheme 1) oxidative addition (OA) of the organic halide substrate into the Pd(0) catalyst generates a square-planar aryl-Pd(II) halide, which undergoes TM with a wide range of organoboron compounds.[5] Reductive elimination (RE) from the diaryl Pd(II) intermediate formed after TM completes the cycle. Improving our mechanistic understanding of TM would enable better catalytic cycle design. Not surprisingly, TM to Pd(II)

intermediates related to the Suzuki-Miyaura catalytic cycle is well studied by experimental[6, 7] and computational[8, 9] mechanistic approaches. Similarly, the catalytic cycle[10] for 1,4-addition of arylboronic acids[11] (e.g., **1**; Scheme 2) to organic electrophiles such as 2-cyclohexenone (**2**) involves transmetalation to a square-planar Rh(I) centre (Scheme 1). However, experimental studies on Rh transmetalation are scarce.[12] Even though recently a significant attention has been devoted to understanding the enantioselectivity controlling carborhodation step in the 1,4-addition reaction by means of density functional calculations,[13] no exact studies exist for the preceding, turnover-determining transmetalation step.[14, 15]

Following pioneering studies by Miyaura et al. in 1997,[16] the groups of Hayashi and Miyaura jointly presented in 1998[17] the first highly enantioselective 1,4-addition of arylboronic acids mediated by a [(binap)Rh(I)]⁺ catalyst (binap = 2,2′-

Scheme 1. Transmetalation as a common step in important catalytic reactions of late transition metals: Suzuki-Miyaura (left) and Hayashi-Miyaura (right). TM = transmetalation, OA = oxidative addition, RE = reductive elimination, EB = enone binding, CR = carborhodation, EH = (Rh) enolate (oxa-π-allyl) hydrolysis.

Scheme 2. Previously published catalytic asymmetric Hayashi-Miyaura (1,4-addition) reaction. Conditions: 3 mol% (*P*)-**I** + 3 mol% [Rh(acac)(C₂H₄)₂], 100 °C, 5h;[17] 3 mol% (*R*)-**II** +3.3 mol% Rh as [RhCl(C₂H₄)₂]₂, 40 °C, 1.5 h.[18]

bis(diphenylphosphino)-1,1′-binaphthyl, **I**). In the years after, the Hayashi-Miyaura reaction and related Rh(I)-catalyzed arylations[11] have become one of the most important catalytic asymmetric manifolds. In 2003, Hayashi group presented[19] a conceptually novel ligand class,[20] chiral, C_2-symmetric bidentate olefins based on the bicyclo[2.2.2]octa-2,5-diene (bod) framework such as **II**. Simultaneously and independently, Carreira group developed C_1-symmetric derivatives for the Ir-catalyzed π-allyl substitution.[21] Detailed kinetic measurements[22] showed that: 1) the transmetalation is the rate-determining for the whole cycle; and 2) diene ligands are more reactive than diphosphanes: the addition of PhB(OH)$_2$ (**1**) to 2-cyclohexenone (**2**) requires 3 h at 40°C to produce 97% yield of **3** (96%ee) with Phbod as the ligand[18] as opposed to 5 h at 100°C to 93% of **3** (97%ee) with binap with similar excess of **1** (2-2.5 equiv.).[17] These examples demonstrate the importance of transmetalation step for the overall success of the asymmetric arylation. Herein we present a comparative study of transmetalation for ligands **I** and **II** in the course of the asymmetric 1,4-addition reaction.

Results and discussion

Computational methods

Exploration of key stationary points along the potential energy hyper-surface (PEHS) for the transmetalation reaction was performed with Gaussian09 software suite[23] using the standard Perdew-Burke-Ernzerhof generalized gradient approximation (GGA) DFT functional hybrid with 25% Hartree-Fock (HF) exchange (PBE0).[24] The DeGauss full-electron, DFT-optimized basis set designed for low basis set superposition error (BSSE) (DGDZVP)[25] was chosen to build the atomic orbitals. This basis set includes valence shell polarization functions on both heavy atoms and hydrogens and supports quantitative analysis of the electron density distribution by Bader's Atoms-In-Molecules[26] (AIM) method (see below). Structural optimization of minima was performed in implicit 1,4-dioxane employing the integral equation formalism polarisable continuum model (IEFPCM).[27] Structural optimizations cut-off values for Rh complexes were as follows: for maximum force: 0.0001500, root-mean-square (RMS) force: 0.0001000, maximum displacement: 0.001800, and RMS displacement: 0.001200. Transition state search was performed by relaxed potential energy scan of the relevant bonds or dihedral angles in gas phase followed by additional refinement of the transition state guess generated thereby. The final geometry optimization was combined with a frequency calculation (under the harmonic approximation) to: 1) confirm the nature of the stationary point - 0 or 1 negative (imaginary) frequencies for minima and transition states, respectively. 2) obtain the zero-point correction and the vibrational partition function hence ΔG, ΔH and ΔS (under the ideal gas approximation). For reasons of computational efficiency (DFT methods scale roughly to the 3rd power of the basis functions number), detailed characterization of the transmetalation pathways was conducted only for ligand **II**, followed by calculations of the stationary points along only the preferred pathway for ligand **I**. The [(ligand)Rh-OH]+PhB(OH)$_2$ composition requires 508 and 908 basis functions for ligands **II** and **I** , respectively, with DGDZVP basis set. AIM analyzes were performed using AIMAll software suite (version 14.06.21) with the default parameters.[28]

Transmetalation with diene ligands

Transmetalation being a transfer of a Ph residue from Rh to B presupposes the formation of a single entity incorporating these 3 components. In 2004, Miyaura proposed the adduct of M-OH and PhB(OH)$_2$ (neutral for M = Rh(I) and cationic for M = Pd(II), respectively), in which the boron is tetracoordinate, as the key transmetalation intermediate for the 1,4-addition reaction (Figure 1a).[29] The experimental mechanistic studies have established that the active catalyst most likely is the [(L)Rh(OH)] (L = bidentate ligand) species, which is sufficiently basic to quarternize PhB(OH)$_2$ giving rise to the Miyaura's proposed intermediate. This is consistent with the experimental observation that the reaction proceeds to completion even without adding an external base.[17, 30] Initial modelling of PhB(OH)$_2$ showed that there are 3 conformations which can be distinguished by the position of the H atom relative to the Ph ring - on the same (in) or the opposite (out) side across the B-OH bond (Figure 1b). The "in/out" conformation (**1a**) is the most stable. Expecting this stabilization to be at least partially preserved along the pathway, we restricted our study to this conformation only for reasons of computational efficiency. The initial association in the TM profile (Figure 1c, **4-12**) gives rise to an H-bonded adduct (**5**) of the catalyst [((S)-**II**)Rh(OH)] (**4**) and **1a**. Because the two OH groups in **1a** are non-equivalent, there are two possible pathways depending on whether the "in" or the "out" OH group is engaged. The H-bond is confirmed by the AIM analyses of the electron density finding BCPs between O_1 and H_2 ($\rho_b = 0.0669$ for **5a** and 0.0743 for **5b**; for comparison, the ρ_b for the O_1-H_1 "whole" bond are 0.3442 and 0.3433, respectively) (Figure 2). The H-bond formation is accompanied by lengthening of the Rh-O_1 distance from 1.981 Å in **4** to 2.051 Å in **5a** and 2.047 Å in **5b**, respectively. The H-bond bond length (H_2-O_1) is 1.560 Å in **5a** and 1.505Å in **5b**. In the initial adduct in the "in" pathway (**5a**), a weak interaction between Rh and C_2 ($\rho_b = 0.0443$) was detected by AIM analysis (compare to $\rho_b = 0.1248$ for the Rh-C_1 bond in **11**). The Rh-C_2 distance is 2.444 Å. In contrast, the analogous "out" structure **5b** has the second B-OH group weakly coordinating ($\rho_b = 0.0562$) the Rh centre positioned 2.229 Å away. Structure **5b** is considerably more stable than **5a** (ΔG = −11.1 vs. −6.0 kcal mol^{-1}, respectively). The pathway continues by activation of PhB(OH)$_2$ by the Rh-bound OH group executed by a sliding/rotating motion of the B centre towards O_1. The respective TSs for this step (**6**) are much closer in energy, with the "out" structure (**6b**) being higher in energy than the "in" (**6a**) (ΔG = 4.4 vs. 3.0 kcal mol^{-1}, respectively). The barrier for the "out" activation is 15.5 kcal mol^{-1} compared to 10.4 kcal mol^{-1} for the "in". It appears that a Curtin-Hammett situation is in place: the less stable intermediate (**5a**) reacts faster. TS **6a** collapses to intermediate **9a**. The B-O_1 distance shortens from 3.226 to 2.388 Å to 2.541 Å going in the sequence **5a→6a→9a**. In **6a**, the H-bond is replaced by a weak O_1-B interaction ($\rho_b = 0.0266$), which strengthens in **9a** ($\rho_b = 0.1829$), corresponding to the new B-O bond. In the intermediate **9a**, the weak Rh-C_2 interaction is replaced by a new Rh-C_1 weak ($\rho_b = 0.0546$) interaction as a consequence of the slight rotation of **1b** in the sequence **5a→6a→9a**. In the first intermediate of the "out" pathway (**5b**), PhB(OH)$_2$ lies in the plane of the Rh coordination square. The

quarternization of the boron from planar (sp^2) to tetrahedral (sp^3) upon attack by the Rh-bound OH causes the Ph ring to turn out of this plane. TS **6b** collapses to the intermediate **7**, in which two OH groups coordinate Rh centre. The Rh-O distances are
5 virtually identical (2.134 and 2.133 Å) and PhB(OH)$_2$ is almost symmetrical with respect to the diene ligand: the diene CH$_2$-CH$_2$ bridge and the B-C$_1$ bond are perfectly aligned yet the Ph ring is slightly tiled due to avoiding the clash with the Ph ring on the chiral diene ligand. This is confirmed by the equal bond lengths
10 and electron densities (2.133 and 2.134 Å, and ρ_b = 0.0769 and 0.0758 for Rh-O$_1$ and Rh-O$_3$, respectively). In this structure, the Ph group sits perpendicularly to the Rh coordination plane occupied by the two diene and two OH groups. Attempts to locate a Ph transfer TS from this structure showed that conformational
15 rearrangement via rotation around the Rh-O$_1$ bond, which moves the Ph group in the coordination plane, is preferred. In view of the importance of this process , we located the corresponding torsional TS **8** (ΔG = −2.5 kcal mol^{-1}), wherein O$_3$ moves out and the Ph group moves in the Rh coordination site. Accordingly, the
20 Rh-O$_3$ bond lengthens from 2.134 (in **7**) to 2.574 Å; the corresponding loss of bonding is evident by comparing the ρ_b value decreasing from 0.0758 (in **7**) to 0.0322. TS **8** collapses to intermediate **9b**, very similar to the corresponding intermediate on the "in" pathway (**9a**) produced directly by collapse of TS **6a**,
25 with exception of the conformation of the free OH groups of PhB(OH)$_2$. The Rh-O$_1$-B-C$_1$ dihedral angle value at TS **8** (−54°) is strongly supportive of the torsional nature of this stationary point. Both "in" and "out" pathways converge into a single B-to-Rh TS (**10**), which is considerably higher in energy than **8** (ΔG =

30 2.0 kcal mol^{-1}). TS **10** collapses to a Rh-Ph intermediate (**11**), in which a B(OH)$_3$ molecule is coordinated to the Rh centre. AIM analysis shows that attaching the electron-poor B(OH)$_2$ fragment diminishes the ρ_b value from 0.1138 in **4** to 0.0769 in **11**, suggesting weaker coordination also confirmed by the
35 lengthening of the Rh-O$_1$ bond from 1.981 to 2.317 Å, respectively. Surprisingly, the B-to-Rh transfer is almost energetically neutral (ΔG = −9.2 and −9.4 kcal mol^{-1}for **9a** and **11**, respectively). TS-less dissociation of B(OH)$_3$ (**13**) completes the TM sequence, giving a tricoordinate Rh-Ph intermediate **12**,
40 which is free to coordinate an acceptor molecule such as **2** and continue the reaction. ΔG drops by a net of 2.8 kcal mol^{-1} to −12.2 kcal mol^{-1} balancing out the large loss of Rh-O(H)-B(OH)$_2$ coordination energy (ΔH term is highly endothermic, from −21.1 to −12.4 kcal mol^{-1}) with an even larger entropy gain. In **11**, two
45 of the **3** hydrogen atoms adopt *syn* conformation (**13a**). The alternative conformation **13b**, in which all 3 H atoms are mutually "*anti*" is considerably more stable (by 4.0 kcal mol^{-1}). Factoring this conformational stabilization in lowers the total ΔG of the TM sequence to −16.2 kcal mol^{-1}.
50 Overall, the energies of the TS suggest that: 1) the "in" pathway having the smallest energy span is preferred , and; 2) TS **8** provides a low energy switch from the "out" into the "in" pathway. Progressing along the reaction coordinate, the Rh-C$_1$ distance grows progressively shorter: in the "in" pathway,
55 2.728→2.505→2.356→2.188→2.040 →2.006 Å in the sequence **5a→6a→9a→10→11→12**; in the "out" pathway, 4.746→4.152→3.643→2.634→2.407 Å in the sequence **5b→6b→7→8→9b**. Similarly, the B-C$_1$ distance grows
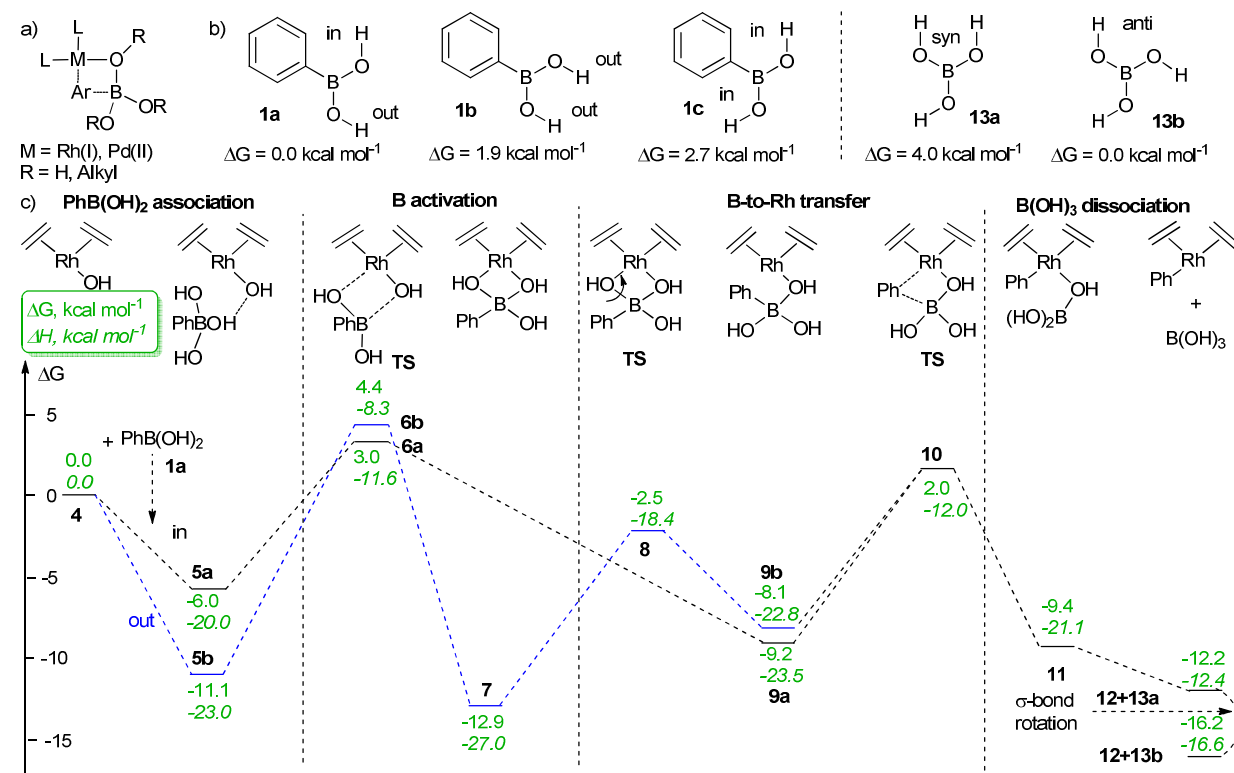

60 **Figure 1.** (a) The putative transmetalation intermediate ('Miyaura's intermediate'). (b) Conformations of the PhB(OH)$_2$ (**1a-c**) and B(OH)$_3$ (**13a,b**) and their relative energies (PCM(1,4-dioxane, 303.15 K)/PBE0/DGDZVP level of theory). (c) The transmetalation reaction profile (the same level of theory) showing ΔG and ΔH (italics) of stationary points (in green) relative to the sums of the corresponding values for **4** and **1b**. The reaction coordinate is shown schematically at the top.
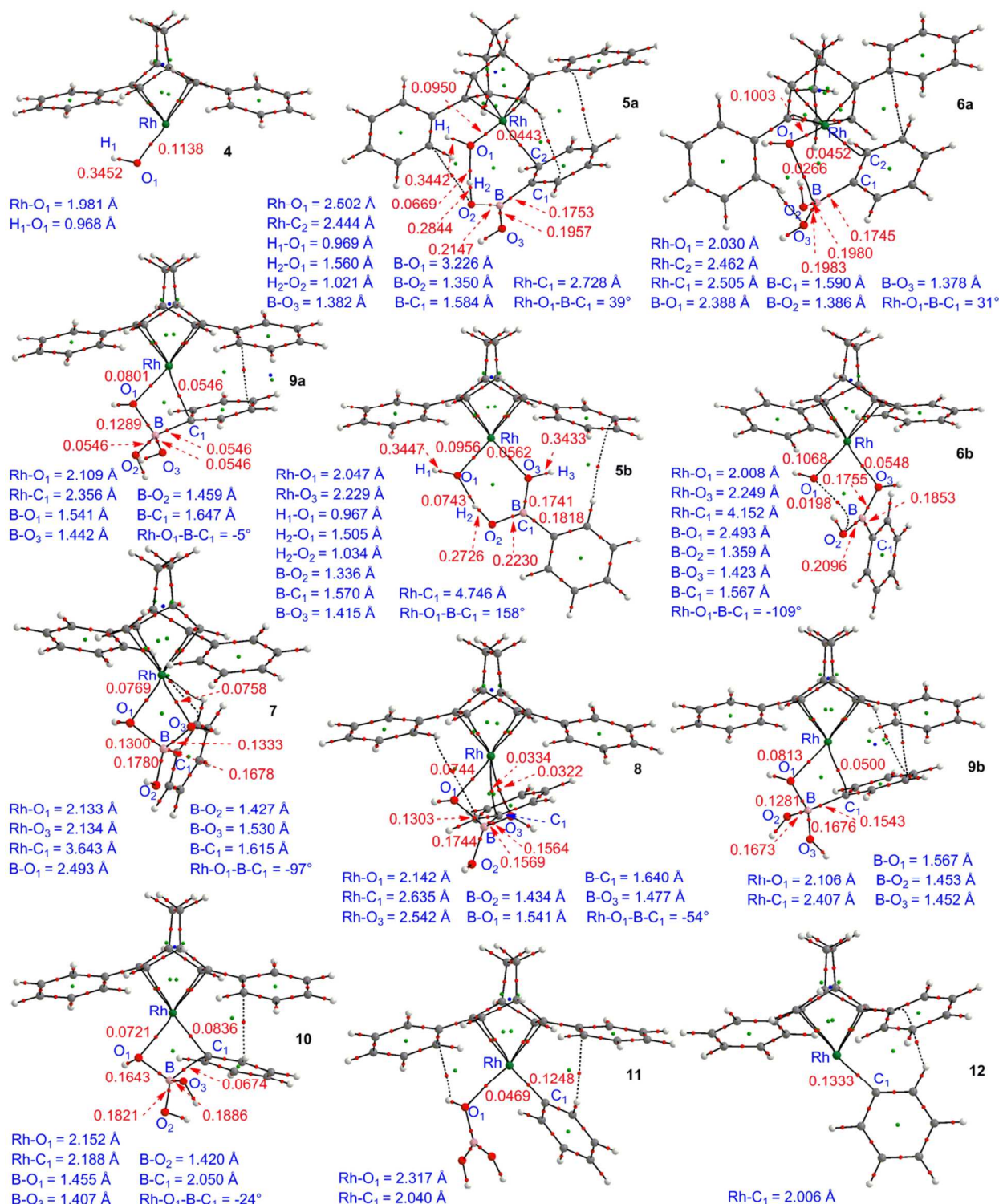
Figure 2. AIM plots (PCM(1,4-dioxane)/PBE0/DGDZVP level of theory) for key stationary points along the reaction coordinate in the transmetalation reaction profile (Figure 1). The critical points (CP) are shown as follows: bond (B), in red; ring, in green; cage, in blue. Selected BCP ρ_b values (red), bond lengths, bond angles and torsional angles (blue) are also shown.

progressively longer: in the "in" pathway, $1.584 \rightarrow 1.590 \rightarrow 1.647 \rightarrow 2.050 \rightarrow 3.128 \rightarrow \infty$ Å in the sequence **5a→6a→9a→10→11→12**; in the "out" pathway, $1.570 \rightarrow 1.567 \rightarrow 1.615 \rightarrow 1.640 \rightarrow 1.644$ Å in the sequence **5b→6b→7→8→9b**. The "in" pathway from the very beginning delivers the Ph-B group in the correct orientation hence the

overall distance travelled by the reacting atoms is smaller than in the alternative "out" pathway. This motion is ultimately governed by the key Rh-O_1-B-C_1 dihedral angle (D1). Due to the C_2 ligand symmetry, only two, pathway-determining alternatives − *syn* for "in" (Ph group in the Rh coordination plane) vs. *anti* for "out" (Ph group perpendicular to the Rh coordination plane) − are possible,

as it can be most clearly seen in 'Miyaura intermediate' **6**. Along the pathway, D1 adopts values 39→31→−5→−24° in the sequence **5a→6a→9a→10**. and 158→−109→−97→−54→4→−24° in the sequence
5 **5b→6b→7→8→9b→10**.

Transmetalation in the presence of a Rh-coordinated water molecule

The active catalyst [(L)Rh(OH)] has been shown to exist in fast equilibrium with the corresponding tetracoordinate μ-OH
10 dimer.[22] Conceivably, a water molecule from the water co-solvent can act as the 4th ligand, forming an aqua complex of the type [(L)Rh(OH)(OH$_2$)].[22] It is to be expected that the aqua complex formation will have an effect on the subsequent transmetalation step. Therefore, we calculated the transmetalation mechanism in
15 the presence (Figure 3, **14-21**) of a σ-coordinated water molecule. For the (*S*)-Phbod ligand ((*S*)-**II**), the tri-coordinate [((*S*)-**II**)Rh(OH)] (**4**) is 6.0 kcal mol^{-1} less stable than the corresponding tetracoordinate, square-planar aqua complex **14**. The presence of the water molecule in the coordination sphere of
20 the metal complicates the profile by lowering of the symmetry. This in turn affects the number of possible profiles expressed by the number of unique conformations arising from rotation around the D1 coordinate. This effect is easiest to discern in the quarternized PhB(OH)$_2$ **17** ('Miyaura's intermediate'). Total of 3
25 conformers were found: **17a** (ΔG = −12.9 kcal mol^{-1}) having D1 value of −13° (conf1), **17b** (ΔG = −12.2 kcal mol^{-1}) having D1

value of 62° (conf2), and **17c** (ΔG = −11.3 kcal mol^{-1}) having D1 value of −178° (conf3). These 3 conformers lie on the reaction coordinates of 3 pathways, which will be referred to in analogous
30 manner, "conf1", "conf2" and "conf3". In **17a**, Rh is coordinated with O$_1$ and C$_1$(Ph) whereas in **17b** and **c**, with O$_1$ and O$_2$. The Rh-O$_1$ bond lengths are almost identical in the 3 structures (2.131, 2.127, and 2.136 Å for **17a**, **b**, and **c**, respectively) (Figure 4). The Rh-C$_1$ bond length in **17a** is 2.362 Å. The Rh-
35 coordinated H$_2$O molecule (Rh-O$_2$ bond lengths 2.183 and 2.193 Å in 17**b** and **c**, respectively) engages in additional H-bonding with one of the two B-OH groups forming a 7-membered chelate. The H-atom of H$_2$O positioned closer to Rh (H$_3$) acts as the donor and O$_3$ - as the acceptor; the corresponding H$_3$-O$_3$ distances are
40 1.551 and 1.559 Å. In contrast, the H$_2$O molecule is displaced from the coordination sphere of the metal by **1a** forming a 5-member chelate with O$_1$ and C$_1$ atoms. However, the H$_2$O molecule still does not leave the scene by forming an analogous H$_3$ (donor)⋯O$_3$ (acceptor) H-bond (O$_3$-H$_3$ inter-atomic distance
45 is 1.818 Å). The "Miyaura's intermediates" **17a**, **b**, and **c** are produced upon the collapse of the quarternization TS **16a**, **b**, and **c** for "conf1", "conf2" and "conf3" pathways, respectively. The B-O$_1$ bonds in the TSs are considerably longer (2.760, 2.647, and 2.760 Å in **16a**, **b**, and **c**, respectively) than in the intermediates
50 that follow (1.539, 1.541, and 1.527 Å in **17a**, **b**, and **c**, respectively). In the "conf1" pathway, the H$_2$O molecule is still coordinated to Rh (Rh-O$_2$ bond length of 2.220 Å) and the
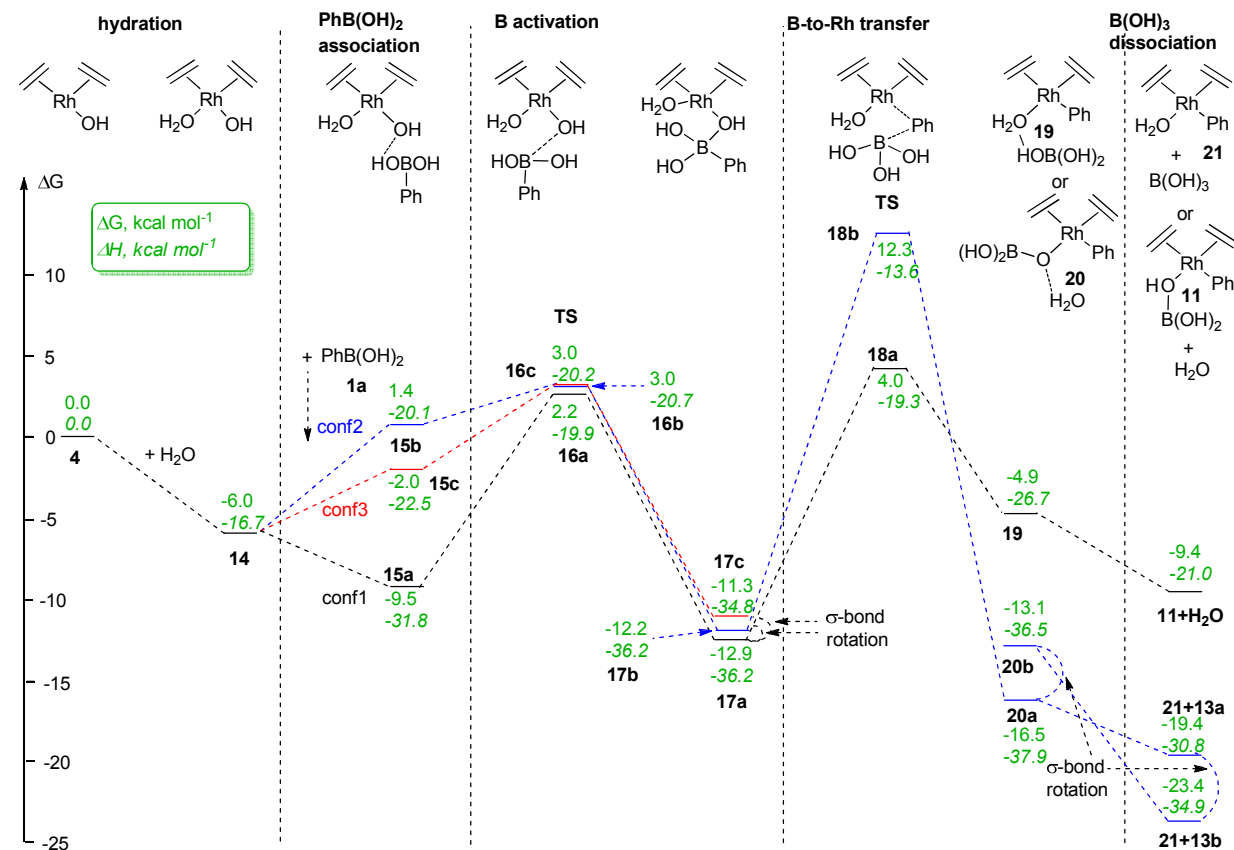

Figure 3. An alternative transmetalation reaction profile (PCM(1,4-dioxane, 303.15 K)/PBE0/DGDZVP level of theory) to account for Rh(I) aqua
55 complex formation showing ΔG and ΔH (italics) of stationary points (in green) relative to the sums of the corresponding values for **4**, **1b**, and H$_2$O. The reaction coordinate is shown schematically at the top.
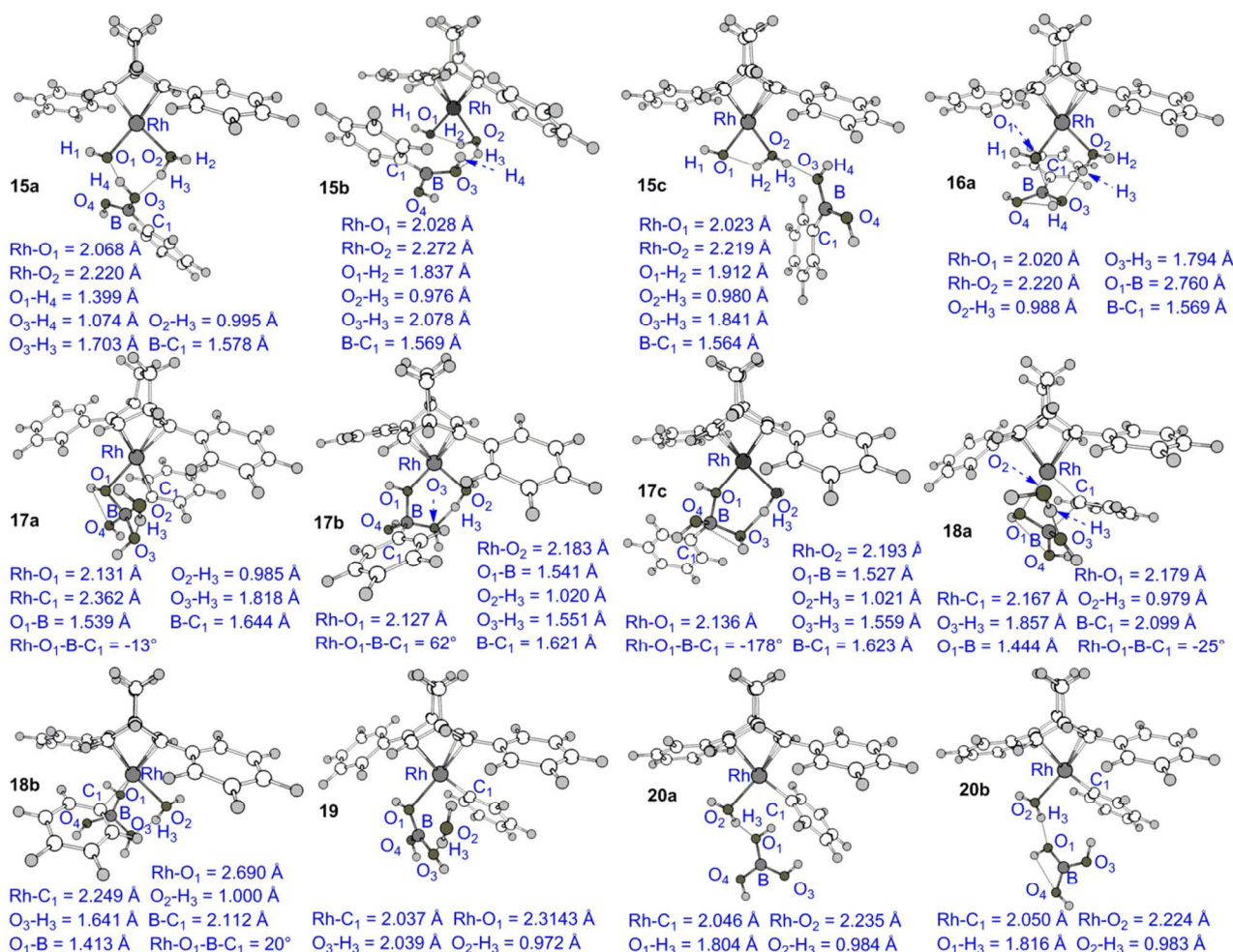
Figure 4. Structure plots (PCM(1,4-dioxane)/PBE0/DGDZVP level of theory) for selected key stationary points along the reaction coordinate in the hydrated transmetalation reaction profile (Figure 3). Selected bond lengths, bond angles and torsional angles (blue) are shown.

$H_3 \cdots O_3$ H-bond persists (bond length of 1.736 Å). That signifies that B quarternization in the "conf1" pathway proceeds with an expulsion of H_2O molecule from the coordination sphere of the metal. The H-bonding pattern is considerably rearranged in the "conf2" and "conf3" pathways. In the first case, there are two H bonds, $H_2 \cdots O_1$ (bond length of 1.846 Å) and $H_3 \cdots O_3$ (bond length of 2.082 Å). In the second case, there are two analogous H bonds, $H_2 \cdots O_1$ (bond length of 1.909 Å) and $H_3 \cdots O_3$ (bond length of 1.987 Å). TSs **16** arise from the initial adducts **15**. The complex **15a** in the "conf1" pathway features a 6-membered chelate network tightly held together by two rather short H-bonds, $H_4 \cdots O_1$ (bond length of 1.399 Å) and $H_3 \cdots O_3$ (bond length of 1.703 Å). In the sliding motion that takes place during the B quarternization, the $H_4 \cdots O_1$ H bond is lost due to the O_1 atom sliding forward and the $O_3 \cdots H_4$ bond rotating out. The second H-bond persists into the TS **16a** and onto the subsequent intermediate **17a**. On the other hand, in the other two pathways the original active catalyst hydrate structure (**14**) is largely preserved upon coordination of PhB(OH)$_2$. In **14**, the Rh-O$_1$ (the anionic oxygen) bond length is 2.038 Å and the Rh-O$_2$ (the neutral oxygen) bond length is 2.251 Å, as expected. The H atom on the water molecule which is proximal to the hydroxide (H_2) is H-bonded to the latter (1.769 Å). The H-bond causes a lengthening of the $O_2 \cdots H_2$ bond (0.996 Å) compared to the

$O_2 \cdots H_3$ bond (0.969 Å). Going to **15b** and **15c**, one of the oxygen atoms from PhB(OH)$_2$ forms a H-bond with H_3 (bond lengths 2.078 and 1.841 Å in **15b** and **c**, respectively). There is a major topological difference between the two intermediates in the sense than in **15b** the PhB(OH)$_2$ is "wrapped around" the Rh centre, whereas in **15c** it is extended out.

Continuing from **17**, B-to-Rh transfer takes place. This is not possible from "conf3", because the Ph group is on the opposite side of the Rh atom; from this conformation, the pathway merges with either conf1 or conf2 via rotation around the key D1 torsional angle. As it was demonstrated earlier, this conformational change is expected to be at least 3-4 kcal mol^{-1} lower than the ensuing TS **18**, hence the corresponding torsional TSs were not calculated. The conf1 pathway proceeds via TS **18a**, which is an identical structural analogue of TS **10**, with exception of a water molecule H-bonded to the nascent B(OH)$_3$ molecule; the $O_3 \cdots H_3$ distance being 1.857 Å. The Rh-C$_1$ and B-C$_1$ bond lengths are 2.167 and 2.099 Å, respectively, very similar to those in TS **10**. Interestingly, for "conf2" pathway a separate Rh-to-B transfer TS (**18b**) was found, with the transfer occurring at ~30° angle to the Rh coordination plane. In this TS, the water molecule, just as in the structures preceding it, maintains coordination to Rh; the Rh-O$_2$ bond length is 2.218 Å. The B atom is also located at ~30° angle from the Rh coordination plane

on the opposite side to Ph. The Rh-C$_1$ and B-C$_1$ bond lengths are 2.249 and 2.116 Å, respectively. The H$_3$···O$_3$ bond is rather short (1.641 Å). TSs **18** collapse to Rh-Ph species additionally coordinated with H$_2$O ("conf1") or B(OH)$_3$ ("conf2"). The third
5 particle, B(OH)$_3$ and H$_2$O in each respective case is only attached by an H bond and is expected to dissociate with diffusion-controlled rate. In the "conf1" pathway, this produces **11** from the non-hydrated pathway, that is, the two pathways merge herein. In the case of "conf2", a new [((*S*)-**II**)Rh(OH$_2$)Ph] complex (**21**) is
10 produced; the Rh-C$_1$ bond is 2.044 Å, and the Rh-O$_2$ bond is 2.249 Å. Just as in the non-hydrated pathway, a conformational change in B(OH)$_3$ from "syn" (**13a**) to "anti" (**13b**) conformation lowers the end-point ΔG by 4.0 kcal mol^{-1}. Interestingly, if analogous conformational change takes place in the preceding
15 intermediate (**20a** to **20b**), it actually leads to increase of ΔG by 3.4 kcal mol^{-1}.

An overall assessment of the hydrated profile reveals two important points. First, within the hydrated profile, the "conf1" pathway, which is the most structurally similar to the non-
20 hydrated profile "in" pathway, is the most thermodynamically preferred by virtue of having the lowest free-energy span. Second, the barriers within the hydrated profile are significantly higher but the intermediates are significantly lower in energy than the non-hydrated one. This implies that the transmetalation
25 proceeds by the non-hydrated profile, with the hydrated intermediates acting as off-cycle intermediates being in rapid equilibrium with their non-hydrated counterparts. This can be rationalized by considering that from the 4 coordination sites available, 2 are permanently locked by the diene ligand, and two
30 are needed to accommodate Ph and B(OH)$_3$, hence the "dehydrating" of the hydrated pathway by expulsion of a water molecule from the coordination sphere of the metal in the sequence **15a→16a→17a**.

Transmetalation of BINAP-Rh catalysis

35 Having established the validity of the non-hydrated "in" pathway as the main transmetalation mechanism, we calculated this pathway for the classic [Rh(binap)] catalyst (Figure 5a).
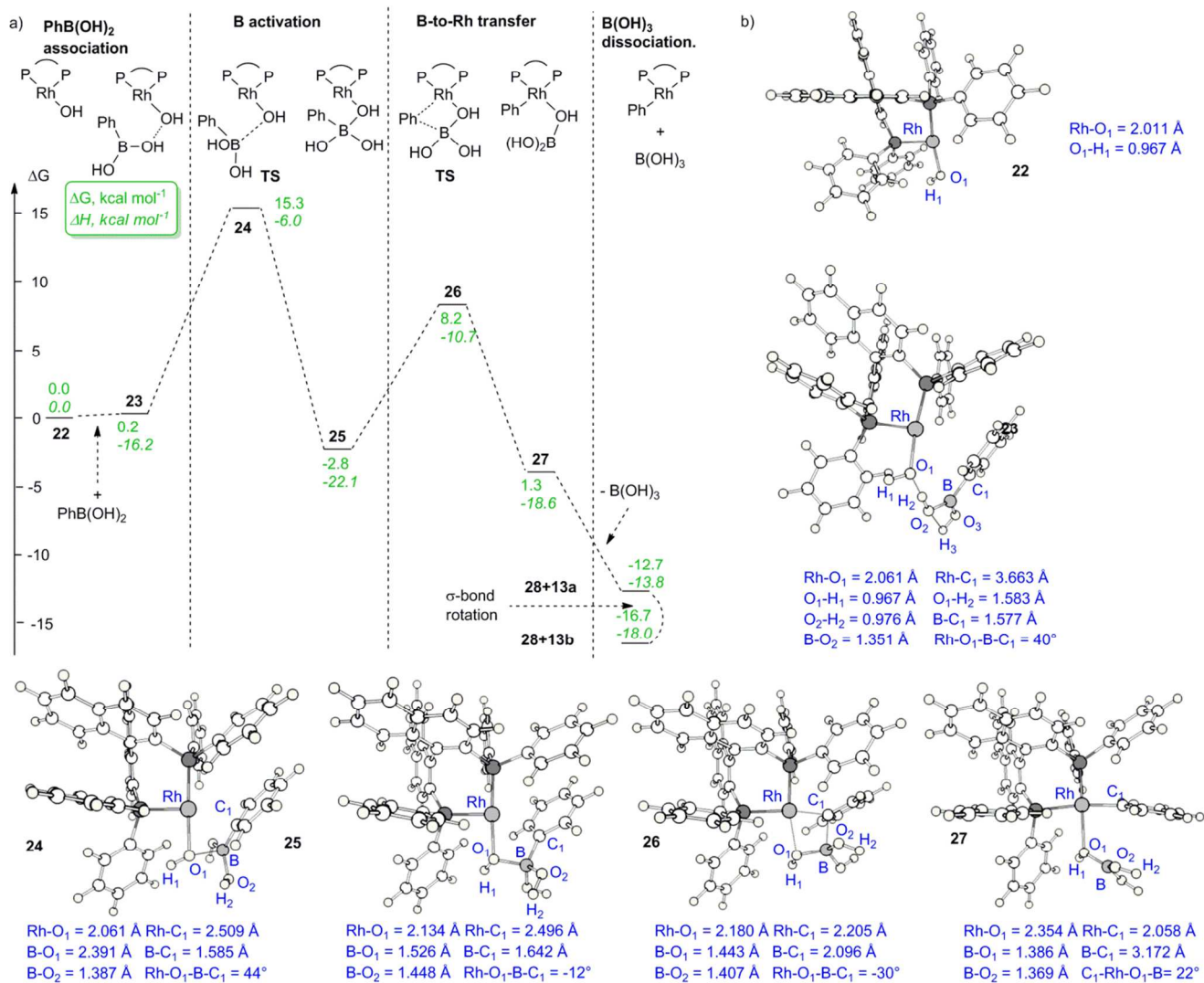

Figure 5. a) The transmetalation reaction profile (PCM(1,4-dioxane, 373.15 K)/PBE0/DGDZVP level of theory) showing ΔG and ΔH (italics) of
40 stationary points (in green) relative to the sums of the corresponding values for **22** and **1b**. The reaction coordinate is shown schematically at the top. b) Structural plots for selected key stationary points along the reaction coordinate at the same level of theory. Selected bond lengths, bond angles and torsional angles (blue) are shown.

ARTICLE TYPE

Comparison of the stationary points Gibbs energies across the pathway reveals important differences. The barriers for both phenylboronic acid activation and B-to-Rh transfer are much higher for the bulker binap ligand than for the smaller Phbod, especially the former (ΔG for TSs **24** and **6a** are 15.3 vs. 4.4 kcal mol⁻¹, respectively). This destabilization persists also in the intermediates on either side of this TS (**23** and **25**), being considerably more endergonic for ligand **I** than **II**. This effect is counter-intuitive considering that the boron activation occurs relatively far from the ligand bulk and the basicity of the Rh-bound OH is expected to be enhanced due to the higher σ-donating power of the phosphane. Comparison of the ΔH values reveals that this effect is due primarily to the entropy term. Similar, but smaller effect occurs at the B-to-Rh transfer TS (ΔG for **10** vs. **26** are 2.0 and 8.2 kcal mol⁻¹, respectively). The ligand change does not affect the reaction thermodynamically, however, ΔG being −16.7 and −16.2 kcal mol⁻¹ for ligands **I** and **II**, respectively. The −TΔS term at this point is close to 0, which strengthens the argument of entropy-lowered transmetalation rate for **I**. The computations, therefore, agree well with the experimentally observed slower reaction rate (attributed to slower transmetalation) for Rh-catalysts carrying ligand **I** vs. **II**. However it should be pointed out that a direct comparison between ligands **I** and **II** is difficult due to the very different reaction conditions (absence and presence of an external base, respectively). Accurate kinetic studies have shown that under the same conditions, the 1,4-addition to methyl vinyl ketone, a very active substrate, catalyzed by [(binap)RhOH] is just 1 order of magnitude slower than when catalyzed by [(cod)RhOH] (cod = 1,5-cyclooctadiene) (rate constants 6.7 and 0.5 M⁻¹ s⁻¹ at 50°C).[22b] Considering Phbod is considerably more sterically congested than cod, the approximately equal B-to-Rh transfer barriers (10.4 vs. 11.0 kcal mol⁻¹) for ligands **II** and **I** predicted by the computation are not surprising.

Structurally, the stationary points are very similar for both ligands (Figure 5b). For the pre-complexed reactants, the O₁···H₂ H-bond length is 1.583 Å in **23** vs. 1.560 in **5a**. Going into the B activation TS, this is replaced by a O₁-B bond having length of 2.391 Å in **24** and 2.388 Å in **6a**; the B-C₁ bonds are 1.585 and 1.590 Å, respectively. In the B-to-Rh transfer TS, the B-C₁ bonds become 2.096 and 2.050 Å, and the Rh-C₁ bonds become 2.205 and 2.188 Å in **26** and **10**, respectively.

The favourable energetics for the non-hydrated "in" pathway for both ligands lends a strong first principles support to 'Miyaura's intermediate' (Figure 1a) in the most typical case of Rh-catalyzed 1,4-addition reaction. Recent work by Lan has shown analogous B-to-Rh pathway in their study of the [(cod)Rh]-mediated C-Si bond scission reaction.[14] Earlier, de Bruin and co-workers performed a computational study of the aldehyde arylation under anhydrous conditions.[15] The results obtained herein, which include effect of water co-solvent as well as treatment of the full ligand structures (and not just two PH₃ particles), are in excellent qualitative agreement. On the other hand, the group of Gois computationally demonstrated that in a similar reaction catalyzed by a N-heterocyclic carbene-Rh₂(OAc)₄ complex, there is no transmetalation; rather, the Rh catalyst assists with boronic acid activation, which then engages in a direct nucleophilic attack on the aldehyde activated by an H-bond.[31] Houk et al. found a structure representing the Pd 'Miyaura's intermediate' in their theoretical investigation of the [(bipy)Pd(OMe)]-catalyzed 1,4-addition (bipy=2,2′-bipyridyl) to 3-methyl-2-cyclohexenone.[32] Whereas no direct experimental support has been provided to date for Rh arylations, Hartwig et al. demonstrated[12] that isolated [(Et₃P)₂Rh-O-B(R)Ar] (R = OH or Ar) underwent B-to-Rh aryl transfer upon heating while producing a boron-containing polymer instead of B(OH)₃; no hypervalent B compounds were detected. Also, kinetic experiments[7] as well as very recent DFT calculations[8] have established the viability of analogous [Ar-Pd(II)-OH] species in Suzuki-Miyaura cross-couplings.

Conclusions

Exploration of the transmetalation of phenylboronic acid to Rh(I)-hydroxide ligated with a chiral bidentate phosphane (binap) and a chiral diene (Phbod) by DFT calculations (IEFPCM/PBE0/DGDZVP level of theory) reveals a two step process comprised of boron activation by the Rh-bonded OH group followed by a B-to-Rh transfer. Whereas the barriers associated with the TSs for both steps were of approximately equal height for Phbod, the first one was much higher for binap. This difference is predominantly entropic in nature. The computations agree well with the experimental findings that transmetalation for [Rh(binap)] is slower than [Rh(Phbod)] and lend first principles support to the "Miyaura's intermediate" postulated in 2004 to arise from quarternization of the boronic acid by Pd(II) or Rh(I)-bound hydroxide.

Notes and references

ᵃ School of Chemistry and Chemical Engineering, Hefei University of Technology, 193 Tunxi Road, Hefei 230009, China. Fax: ++86-551-6290-1450; Tel: ++86-551-6290-1450; E-mail: liyg@hfut.edu.cn, ekantchev@hfut.edu.cn, ekantchev@gmail.com

ᵇ School of Chemistry, Chemical Engineering and Biological Science, Wuhan University of Technology, 205 Luoshi Road, Wuhan, 430070, China

c Former address: Institute of Materials Research and Engineering, 3 Research Link, Singapore 117602

† Electronic Supplementary Information (ESI) available: Cartesian coordinates, energies and first 3 frequencies for all stationary points and
5 IRC plots for selected transition states. See DOI: 10.1039/b000000x/

1. D. G. Hall, ed., *Boronic acids*, 2 edn., John Wiley & Sons, New York, NY, 2012.
2. N. Miyaura, *Bull. Chem. Soc. Jpn.*, 2008, **81**, 1535-1553.
3. D. V. Partyka, *Chem. Rev.*, 2011, **111**, 1529-1595.
10 4. (a) N. Miyaura and A. Suzuki, *Chem. Rev.*, 1995, **95**, 2457-2483; (b) N. Miyaura, K. Yamada and A. Suzuki, *Tetrahedron Lett.*, 1979, **20**, 3437-3440.
5. (a) A. J. J. Lennox and G. C. Lloyd-Jones, *Chem. Soc. Rev.*, 2014, **43**, 412-443; (b) A. J. J. Lennox and G. C. Lloyd-Jones, *Angew. Chem., Int. Ed.*, 2013, **52**, 7362-7370.
6. (a) A. R. Kapdi, G. Dhangar, J. L. Serrano, J. Pérez, L. Garciá and I. J. S. Fairlamb, *Chem. Commun.*, 2014, **50**, 9859-9861; (b) B. Crociani, S. Antonaroli, A. Marini, U. Matteoli and A. Scrivanti; Y. Nishihara, H. Onodera and K. Osakada, *Chem. Commun.*, 2004, **40**,
20 192-193.
7. (a) C. Amatore, G. Le Duc and A. Jutand, *Chem. Eur. J.*, 2013, **19**, 10082-10093; (b) B. P. Carrow and J. F. Hartwig, *J. Am. Chem. Soc.*, 2011, **133**, 2116-2119; (c) C. Amatore, A. Jutand and G. Le Duc, *Chem. Eur. J.*, 2011, **17**, 2492-2503.
25 8. G. Audran, P. Brémond, S. R. A. Marque, D. Siri and M. Santelli, *Tetrahedron*, 2014, **70**, 2272-2279.
9. (a) C.-M. Weng and F.-E. Hong, *Dalton Trans.*, 2011, **40**, 6458-6468; (b) Y.-L. Huang, C.-M. Weng and F.-E. Hong, *Chem. Eur. J.*, 2008, **14**, 4426-4434; (c) A. A. C. Braga, G. Ujaque and F. Maseras,
30 *Organometallics*, 2006, **25**, 3647-3658; (d) A. A. C. Braga, N. H. Morgon, G. Ujaque, A. Lledos and F. Maseras, *J. Organomet. Chem.*, 2006, **691**, 4459-4466; (e) A. A. C. Braga, N. H. Morgon, G. Ujaque and F. Maseras, *J. Am. Chem. Soc.*, 2005, **127**, 9298-9307; (f) J. Jover, N. Fey, M. Purdie, G. C. Lloyd-Jones and J. N. Harvey, *J.*
35 *Mol. Catal. A: Chem.*, 2010, **324**, 39-47.
10. T. Hayashi, M. Takahashi, Y. Takaya and M. Ogasawara, *J. Am. Chem. Soc.*, 2002, **124**, 5052-5058.
11. (a) P. Tian, H.-Q. Dong and G.-Q. Lin, *ACS Catal.*, 2012, **2**, 95-119; (b) T. Hayashi and K. Yamasaki, *Chem. Rev.*, 2003, **103**, 2829-2844;
40 (c) K. Fagnou and M. Lautens, *Chem. Rev.*, 2003, **103**, 169-196.
12. P. Zhao, C. D. Incarvito and J. F. Hartwig, *J. Am. Chem. Soc.*, 2007, **129**, 1876-1877.
13. (a) H.-L. Qin, X.-Q. Chen, Y.-Z. Huang and E. A. B. Kantchev, *Chem. Eur. J.*, 2014, **20**, 12982-12987; (b) E. A. B. Kantchev, *Chem.*
45 *Sci.*, 2013, **4**, 1864-1875; (c) S. Gosiewska, J. A. Raskatov, R. Shintani, T. Hayashi and J. M. Brown, *Chem. Eur. J.*, 2012, **18**, 80-84; (d) E. A. B. Kantchev, *Chem. Commun.*, 2011, **47**, 10969-10971; (e) R. Mariz, A. Poater, M. Gatti, E. Drinkel, J. J. Bürgi, X.-J. Luan, S. Blumentritt, A. Linden, L. Cavallo and R. Dorta, *Chem. Eur. J.*,
50 2010, **16**, 14335-14347; (f) A. Poater, F. Ragone, R. Mariz, R. Dorta and L. Cavallo, *Chem. Eur. J.*, 2010, **16**, 14348-14353.
14. Z. Yu and Y. Lan, *J. Org. Chem.*, 2013, **78**, 11501-11507.
15. A. I. O. Suarez, J. N. H. Reek and B. de Bruin, *J. Mol. Catal. A: Chem.*, 2010, **324**, 24-30.
55 16. M. Sakai, H. Hayashi and N. Miyaura, *Organometallics*, 1997, **16**, 4229-4231.
17. Y. Takaya, M. Ogasawara, T. Hayashi, M. Sakai and N. Miyaura, *J. Am. Chem. Soc.*, 1998, **120**, 5579-5580.
18. G. Berthon-Gelloz and T. Hayashi, *J. Org. Chem.*, 2006, **71**, 8957-
60 8960.
19. T. Hayashi, K. Ueyama, N. Tokunaga and K. Yoshida, *J. Am. Chem. Soc.*, 2003, **125**, 11508-11509.
20. R. Shintani and T. Hayashi, *Aldrichimica Acta*, 2009, **42**, 31-38.
21. C. Fischer, C. Defieber, T. Suzuki and E. M. Carreira, *J. Am. Chem.*
65 *Soc.*, 2004, **126**, 1628-1629.
22. (a) A. Kina, H. Iwamura and T. Hayashi, *J. Am. Chem. Soc.*, 2006, **128**, 3904-3905; (b) A. Kina, Y. Yasunara, T. Nishimura, H. Iwamura and T. Hayashi, *Chem. Asian J.*, 2006, **1**, 707-711.
23. M. J. Frisch, G. W. Trucks, H. B. Schlegel, G. E. Scuseria, M. A.
70 Robb, J. R. Cheeseman, G. Scalmani, V. Barone, B. Mennucci, G. A. Petersson, H. Nakatsuji, M. Caricato, X. Li, H. P. Hratchian, A. F. Izmaylov, J. Bloino, G. Zheng, J. L. Sonnenberg, M. Hada, M. Ehara, K. Toyota, R. Fukuda, J. Hasegawa, M. Ishida, T. Nakajima, Y. Honda, O. Kitao, H. Nakai, T. Vreven, J. A. Montgomery Jr., J. E.
75 Peralta, F. Ogliaro, M. Bearpark, J. J. Heyd, E. Brothers, K. N. Kudin, V. N. Staroverov, R. Kobayashi, J. Normand, K. Raghavachari, A. Rendell, J. C. Burant, S. S. Iyengar, J. Tomasi, M. Cossi, N. Rega, J. M. Millam, M. Klene, J. E. Knox, J. B. Cross, V. Bakken, C. Adamo, J. Jaramillo, R. Gomperts, R. E. Stratmann, O.
80 Yazyev, A. J. Austin, R. Cammi, C. Pomelli, J. W. Ochterski, R. L. Martin, K. Morokuma, V. G. Zakrzewski, G. A. Voth, P. Salvador, J. J. Dannenberg, S. Dapprich, A. D. Daniels, Ö. Farkas, J. B. Foresman, J. V. Ortiz, J. Cioslowski and D. J. Fox, *Gaussian 09, Revision A.1*, 2009, **Gaussian, Inc.**, Wallingford CT.
85 24. J. P. Perdew, K. Burke and M. Ernzerhof, *Phys. Rev. Lett.*, 1996, **77**, 3685-3868; errata: *ibid.*, 1997, **78**, 1396.
25. N. Godbout, D. R. Salahub, J. Andzelm and E. Wimmer, *Can. J. Chem.*, 1992, **70**, 560-571.
26. R. F. W. Bader, *Atoms in Molecules: A Quantum Theory*, Clarendon
90 Press, Oxford, UK, 1990.
27. J. Tomasi, B. Mennucci and R. Cammi, *Chem. Rev.*, 2005, **105**, 2999-3093 and refs. cited therein.
28. T. A. Keith, *AIMAll (ver. 14. 06. 21),* TK Gristmill Software, Overland Park KS, USA, 2014.
95 29. T. Nishikata, Y. Yamamoto and N. Miyaura, *Organometallics*, 2004, **23**, 4317-4324.
30. R. Itooka, Y. Iguchi and N. Miyaura, *J. Org. Chem.*, 2003, **68**, 6000-6004.
31. A. F. Trindade, P. M. P. Gois, L. F. Veiros, V. André, M. T. Duarte,
100 C. A. M. Afonso, S. Caddick and F. G. N. Cloke, *J. Org. Chem.*, 2008, **73**, 4076-4086.
32. Y. Lan and K. N. Houk, *J. Org. Chem.*, 2011, **76**, 4905-4909

Graphical abstract

Phbod
$\Delta G^{\ddagger}$ = 10.4 kcal/mol (303 K)

binap
$\Delta G^{\ddagger}$ = 11.0 kcal/mol (373 K)
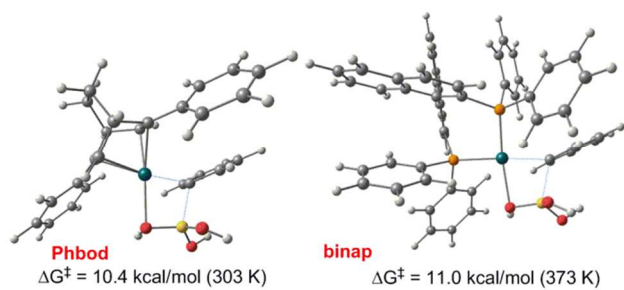
DFT study on the transmetalation of $PhB(OH)_2$ to diphosphane and diene Rh catalysts confirms the propose dintermediate and reactivity trends.